

Phosphorylation-dependent interaction of osteopontin with its receptors regulates macrophage migration and activation

Georg F. Weber,^{*,†} Samer Zawaideh,[‡] Sherry Hikita,[‡] Vikram A. Kumar,^{*} Harvey Cantor,^{*,§} and Samy Ashkar[‡]

[‡]Laboratory for Skeletal Disorders and Rehabilitation, Department of Orthopedic Surgery, Children's Hospital, Harvard Medical School, Longwood Avenue, Boston, Massachusetts; and ^{*}Department of Cancer Immunology & AIDS, Dana-Farber Cancer Institute, and Departments of [†]Medicine and [§]Pathology, Harvard Medical School, Binney Street, Boston, Massachusetts

Abstract: Neutrophil-independent macrophage responses are a prominent part of delayed-type immune and healing processes and depend on T cell-secreted cytokines. An important mediator in this setting is the phosphoprotein osteopontin, whose secretion by activated T cells confers resistance to infection by several intracellular pathogens through recruitment and activation of macrophages. Here, we analyze the structural basis of this activity following cleavage of the phosphoprotein by thrombin into two fragments. An interaction between the C-terminal domain of osteopontin and the receptor CD44 induces macrophage chemotaxis, and engagement of β_3 -integrin receptors by a nonoverlapping N-terminal osteopontin domain induces cell spreading and subsequent activation. Serine phosphorylation of the osteopontin molecule on specific sites is required for functional interaction with integrin but not CD44 receptors. Thus, in addition to regulation of intracellular enzymes and substrates, phosphorylation also regulates the biological activity of secreted cytokines. These data, taken as a whole, indicate that the activities of distinct osteopontin domains are required to coordinate macrophage migration and activation and may bear on incompletely understood mechanisms of delayed-type hypersensitivity, wound healing, and granulomatous disease. *J. Leukoc. Biol.* 72: 752–761; 2002.

Key Words: integrins · delayed-type hypersensitivity · CD44 · metalloproteases

INTRODUCTION

Macrophages participate in two general types of inflammatory reactions. In immediate responses, macrophages are attracted and activated by cytokines secreted from neutrophils and support a reaction that usually is characterized by excessive fibrosis and scar formation. In contrast, delayed-type hypersensitivity responses are largely neutrophil-independent, involve macrophage activation through other cytokines, and include inflammation associated with resistance to infection by

intracellular pathogens and enhancement of wound healing. Differential expression of osteopontin by T cells determines the relative levels of these two responses. Resistance to *Rickettsia* infection, mediated by vigorous induction of osteopontin, leads to an early monocyte influx into infected sites and rapid acquisition of macrophage bacteriocidal activity. Susceptibility to *Rickettsial* infection, on the other hand, reflects delayed and weak osteopontin responses and is characterized by an early accumulation of neutrophils at sites of infection [1, 2]. High levels of osteopontin expression are also a hallmark of monocytic granulomatous reactions in the context of tuberculosis and silicosis [3]. In experimental glomerulonephritis, neutralizing antibodies to osteopontin greatly reduced the influx of macrophages and T cells and reduced kidney damage [4]. Osteopontin may play a central role in bone healing [5, 6], stroke [7], and the revascularization process that is essential for wound healing [8, 9].

Osteopontin has been implicated in cell attachment [10–12] and cell motility [13, 14]. The protein binds to two types of receptors. Engagement of the homing receptor CD44 through a non-RGD cell-binding domain of osteopontin is sufficient to induce chemotaxis or attachment [14, 15]. Binding osteopontin to $\alpha_v\beta_3$ integrin receptors via its Gly-Arg-Gly-Asp-Ser (GRGDS) motif [12, 16, 17] may contribute to osteoclast adherence and resorption of bone [18] as well as to haptotaxis of endothelial cells [19], vascular smooth muscle cells [17, 20], myelomonocytic cells [21], and tumor cells [22]. Vascular smooth muscle cells may also engage osteopontin through $\alpha_v\beta_1$ and $\alpha_v\beta_5$ integrins in an interaction that leads to adhesion of cells but not to migration [13], and adhesion to immobilized osteopontin via integrins α_4 and α_5 has been reported [21]. Engagement of integrin $\alpha_v\beta_1$ may induce migration [23]. Osteopontin is secreted in nonphosphorylated [24–27] and phosphorylated forms [28–30], which contain up to 28 phosphate residues and are differentially induced by tumor promoters and cytokines. Phosphorylation is functionally important, as it may

Corresponding authors: Georg F. Weber, Department of Radiation and Cancer Biology, New England Medical Center, NEMC #824, 750 Washington Street, Boston, MA 02111. E-mail: gweber@lifespan.org; and Samy Ashkar, Children's Hospital, 300 Longwood Avenue, Boston, MA 02115. E-mail: samyashkar@netscape.net

Received January 27, 2002; revised June 5, 2002; accepted June 14, 2002.

determine whether osteopontin associates with the cell surface or with the extracellular matrix [31, 32]. Furthermore, cleavage of osteopontin with thrombin may enhance its cell attachment properties [33]. These results suggest that osteopontin may elicit specific cellular responses depending on its post-translational modification and the cell surface receptor repertoire on its target cell.

The structural basis for the interaction of osteopontin with macrophages leading to migration and perhaps activation is incompletely understood, as earlier studies have often equated function with cell adherence. Prior experiments were performed mostly with cells of different lineages, and it has been shown for other extracellular matrix proteins, including thrombospondin and fibronectin, that their interactions with macrophages could not be predicted from such studies. The necessity for cell attachment of the RGD motif in recombinant osteopontin has been confirmed in mutational analysis. Mutagenesis of the RGD sequence to RAA completely abrogated the interaction of melanoma cells with osteopontin, and mutagenesis of the RGD to RGE resulted in 50% reduction in the attachment of these cells to osteopontin [23]. Mutagenizing the RGD to RGE in mouse osteopontin eliminated the attachment of tumor cells and gingival fibroblasts [34]. Analyses of further structural requirements for osteopontin functions have also demonstrated that phosphorylation may be essential for integrin-mediated cell adhesion [32] and may confer attachment of osteoclasts. It has not been clear whether additional sequences are necessary for osteopontin interaction with its integrin receptors and whether such sequences determine a second binding site or steric modifiers that expose the RGD sequence after phosphorylation. The role of osteopontin phosphorylation in other functions has not been investigated. We have recently found phosphorylation to be essential for various cytokine functions of osteopontin [35–37]. Here, we show that engagement of β_3 -integrin and CD44 receptors by separate domains of osteopontin leads to the expression of distinct macrophage-response phenotypes, which can be separated on the level of biological function, and that the interaction of integrin receptors with osteopontin is regulated by phosphorylation of specific sites on the ligand. We examine macrophages as the cell type that is physiologically predominantly affected by osteopontin, and we compare native osteopontin to recombinant protein that has been phosphorylated on specific sites.

MATERIALS AND METHODS

Cell lines

MH-S is a murine macrophage cell line that was derived by SV40 transformation from an adherent cell-enriched population of alveolar macrophages [CRL-2019, American Type Culture Collection, Manassas, VA (ATCC)]. MT-2/1 is a thymus-derived macrophage from a BALB/c mouse that was immortalized by infection with a retroviral vector [38]. In both cell lines, expression of CD44 and integrin β_3 was measured by flow cytometry with fluorescein isothiocyanate (FITC)-labeled antibodies IM7 and 2C9.G2. CD44 variant expression was analyzed by reverse transcriptase-polymerase chain reaction (RT-PCR) with previously published primer sets [39]. A31 is an integrin $\alpha_3\beta_3^-$, CD44⁻ murine embryonic fibroblast clone derived from BALB/c 3T3 cells (CCL-163, ATCC). A31 cells transfected with CD44 (A31.C1) or A31 mock transfectants were generated as described [14].

Osteopontin purification and cleavage

Recombinant mouse glutathione-S-transferase-osteopontin fusion protein was derived from *Escherichia coli*, digested with factor Xa and purified by affinity chromatography, as described [40, 41]. Osteopontin was purified to homogeneity as determined by N-terminal sequencing. The native osteopontin used in this study was isolated from bone cell cultures or from MC3T3E1 cells and is a full-length protein that is O-glycosylated and highly sialylated, free of sulfate or N-glycosylation, and contains 15–17 phosphate residues. Thrombin cleavage and phosphorylation of the dephosphorylated, native protein or recombinant osteopontin were accomplished by human thrombin (Sigma Chemical Co., St. Louis, MO), protein kinase A, protein kinase G, Golgi kinases, or purified casein kinase II or casein kinase I as described [12, 29, 30, 40–42]. Dephosphorylation was performed using type II potato acid phosphatase [35]. Endotoxin levels of purified osteopontin were below 1 ng/g according to Limulus lysate analysis [35].

In preliminary experiments, MH-S cells attached to but did not spread on phosphorylated and unphosphorylated PNGRGDSLAYGLR synthetic peptides. Therefore, we attempted to isolate a proteolytic fragment that can promote cell spreading. Partial tryptic, chymotryptic, and Asp-N endopeptidase digestion of osteopontin did not result in the isolation of an active peptide; however, a 10-kD fragment was isolated from a Lys-C digest that mediated the spreading of macrophages at approximately 40% (mol/mol) of the activity of the N-terminal thrombin fragment. The N-terminal sequence of this peptide was determined to be QETLPSN. Based on size and sequence analysis of this peptide, referred to as NT10k, we predict that it terminates at the thrombin cleavage site. It contains seven potential phosphorylation sites and approximately 5 mol phosphate/mol peptide. Upon dephosphorylation of this peptide, spreading activity is lost but can be regained by rephosphorylation with Golgi kinases.

Chemotaxis

Directed migration of cells was determined in multiwell chemotaxis chambers [14, 43]. Two-well culture plates (transwell) with polycarbonate filters (pore size 8–12 μm) separating top and bottom wells were coated with 5 μg fibronectin. Cells (2×10^5) were added to the upper chamber and incubated at 37°C in the presence or absence of osteopontin in the lower chamber. After 4 h, the filters were removed, fixed in methanol, and stained with hematoxylin and eosin, and cells that had migrated to various areas of the lower surface were counted microscopically. Controls for chemokinesis included 200 ng of the appropriate form of osteopontin in the top well. For inhibition studies, the cells

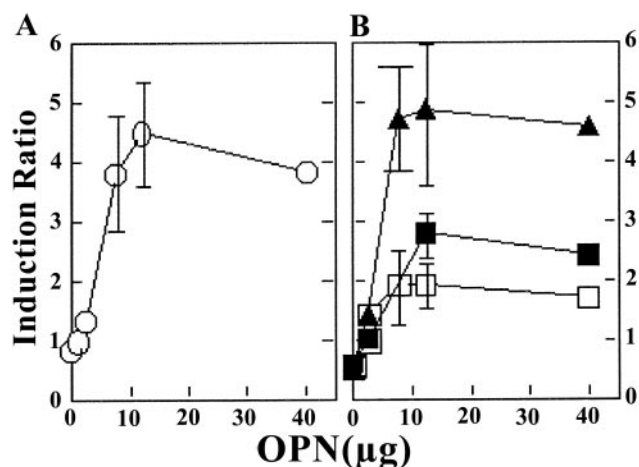


Fig. 1. Titration of osteopontin into the peritoneum induces a cellular infiltrate in a dose-dependent manner. The numbers reflect induction ratios after 6 h of (A) total cells (○) or (B) cells with the surface markers Mac-1⁺ (▲), B220⁺ (■), or CD3⁺ (□) in mice injected with osteopontin versus mice injected with PBS (baseline cell numbers for PBS-injected mice ranged from 443,000 to 1.1×10^6 cells total; 224,000 to 596,000 Mac-1⁺ cells; 31,300 to 176,000 B220⁺ cells; 18,100 to 214,100 CD3⁺ cells). The data points are combined from three experiments. Error bars, where indicated, are mean \pm SE.

were incubated with the relevant antibodies for 15 min before adding to the upper well of the transwell chamber. All assays were done in triplicates and are reported as mean \pm standard error.

Haptotaxis

Haptotaxis of monocytic cell lines to osteopontin or fragments of osteopontin was assayed using a Boyden chamber. The lower surface or both sides of polycarbonate filters with 8 μ m pore size were coated with the indicated amounts of osteopontin. Cells (2×10^5) were added to the upper chamber and incubated at 37°C in the absence of any factors in the lower chamber. After 4 h, the filters were removed, fixed in methanol, and stained with hematoxylin and eosin. Cells that had migrated to the lower surface were counted under a microscope. All assays were done in triplicates and are reported as mean \pm standard error.

In vivo cell migration

Female C57BL/6 mice, purchased from Jackson Laboratories (Bar Harbor, MA) and housed at the Redstone Animal Facility of the Dana-Farber Cancer Institute (Boston, MA), were injected intraperitoneally (i.p.) with 200 μ l phosphate-buffered saline (PBS) containing varying dosages of K7 osteosarcoma-derived osteopontin. Injections of vehicle alone (PBS) served as negative controls. The mice were sacrificed by CO₂ asphyxiation at varying times after injection followed by immediate collection of peritoneal exudate by i.p. injection and recovery of twice 10 mL PBS. Red blood cells were removed by hypotonic lysis with ACK buffer (0.15 M NH₄Cl, 1.0 mM KHCO₃, 0.1 mM Na₂EDTA, pH 7.4) for 5 min at room temperature. Cells were washed and resuspended in Dulbecco's modified Eagle's medium containing 5% fetal bovine serum for fluorescent antibody staining at a concentration of 0.2–1 million cells in 50 μ l. Fluorescence-labeled antibodies (1 μ g/ 1×10^6 cells) were incubated with cells for 30 min at 4°C, before washing twice with 200 μ l PBS and fixation in 500 μ l 2% paraformaldehyde in PBS. Analysis for cellular expression of CD44 (Pgp-1, phycoerythrin) together with CD11b [membrane attach complex (Mac)-1, FITC, macrophage marker], B220 (FITC, B cell marker), or CD3 (FITC, T cell marker) was performed by dual-color flow cytometry with antibodies from PharMingen (San Diego, CA) using a Coulter (Miami, FL) EPICS flow cytometer. Appropriate, nonspecific antibody controls and single-color controls were included.

Cell attachment and spreading

Cell adhesion is a prerequisite for chemotaxis, haptotaxis, and cell spreading. In vitro assays revealed that cells display passive and active adhesion. Active

adhesion is pH- and temperature-dependent, reduced by trypsin treatment, and dependent on cell viability. Passive adherence is temperature- and pH-independent, unaffected by trypsin treatment, and independent of cell viability. Maximal levels of active adherence by macrophages depend on harvest of cells without enzymes from subconfluent cultures and limited exposure to temperature fluctuation. In these studies, we distinguish among cell passive adhesion, active adhesion, and spreading. Passive adhesion is not associated with rearrangement of the cytoskeleton: Attached (possibly adhered) cells cannot undergo G0-G1 transition (as judged by cyclin D expression) and become nonviable within 6–12 h. Actively adherent cells rearrange their cytoskeleton, can undergo G0-G1 transition, and proliferate. Spread cells are arrested cells in G2, do not proliferate, and are characterized by focal adhesion plaques. Most dye-binding assays cannot differentiate these different types of attachment. Dye-binding assays, such as crystal violet, which bind very tightly to dead cells, do not allow differentiation between cell debris and live, actively attached cells.

Twenty-four-well plates were coated overnight at 4°C with 10 μ g/ml of the indicated ligand and were then blocked for 1 h at room temperature with 10 mg/ml bovine serum albumin (BSA) in PBS. At these concentrations, the osteopontin-derived ligands are several orders of magnitude in excess of the estimated numbers of receptors on the plated cells and are considered saturating so that moderate differences in ligand binding to the plastic do not affect the experiment. To preserve the integrity of adhesion receptors, MH-S monocytic cells were harvested from subconfluent cultures by nonenzymatic cell-dissociation solution (Sigma Chemical Co.). The cells were washed twice with PBS and resuspended at a concentration of 1×10^5 cells/ml in sterile Ca²⁺- and Mg²⁺-free PBS supplemented with 0.1% BSA and 1 mM sodium pyruvate. Cells (5×10^4) were incubated in each well, and after 1 h at 37°C, the wells were washed three times with 0.5 ml PBS to remove nonadherent cells, fixed in 1% glutaraldehyde in 0.1 M cacodylate buffer (pH 7.4) at room temperature for 1 h, and were then stained with toluidine blue and hematoxylin. The total number of attached or spread cells in each well was counted microscopically using a Nikon Eclipse microscope equipped with a Sony digital camera. Total number of attached or spread cells was quantitated using Optima 5.2 image analysis system. Each experiment was done in triplicates and is reported as mean \pm standard error. To minimize variability inherent to cell-attachment studies, we scored cells as attached only when a defined nucleus was observed accompanied by a transition from round to cuboidal cell morphology. Round cells are loosely attached with no defined nucleus and were scored as nonattached. These cells can be removed with repeated washes. The viability of the cells was measured before and after the termination of the experiments, and

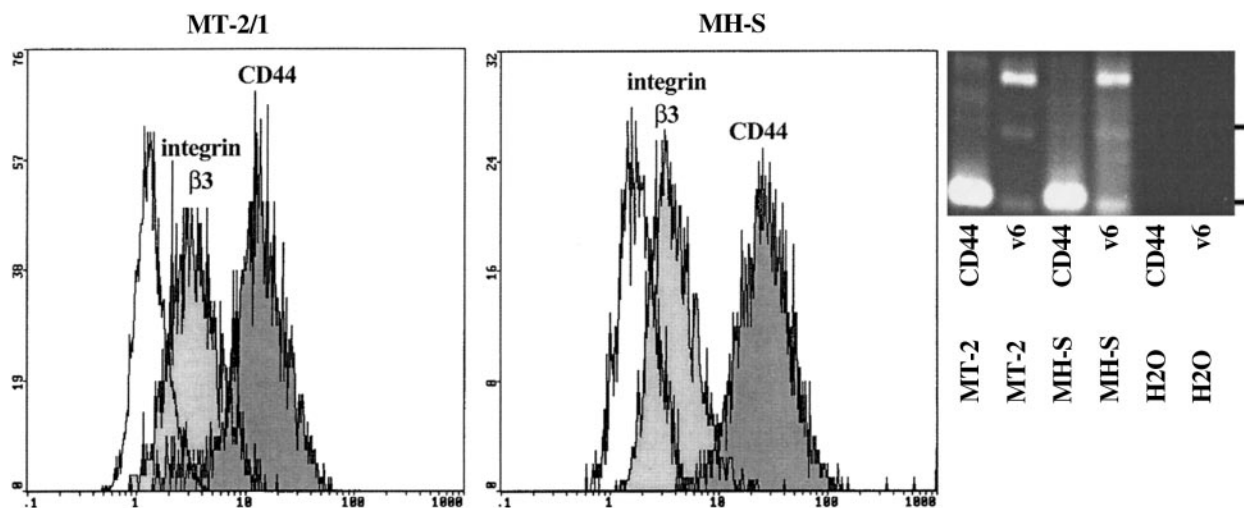


Fig. 2. Expression of CD44 and integrin β_3 by MH-S and MT-2 cells. The expression levels of CD44 and integrin β_3 were measured by flow cytometry with FITC-conjugated antibodies to these surface receptors (anti-pan-CD44 clone IM7 and 2C9.G2) and an irrelevant control antibody (open peak, not labeled). RT-PCR with primers for the constitutive exons 5 and 16 of CD44 (MT-2 CD44 and MH-S CD44) amplifies a prominent band of about 200 bp in macrophage cell lines (with these primers, the standard form would yield a product of 135 bp; ref. [39]), indicating that standard CD44 is not abundantly expressed. RT-PCR with primers for the exons 5 and v6 (MT-2 v6 and MH-S v6) results in three PCR products, ranging in size from 200 bp to 400 bp, corroborating the expression of multiple CD44 variants that contain the exon v6. No bands were seen in the no-template controls (H₂O CD44 and H₂O v6). The two lateral lines indicate the positions of the markers for 194 bp and 300 bp.

TABLE 1. Migratory Activity of Osteopontin and Its Thrombin Fragments

		Lower Chamber			
		PBS	OPN	OPN-CT	OPN-NT
Upper Chamber	PBS	42 ± 8	231 ± 34	389 ± 52	69 ± 9
	OPN	12 ± 5	164 ± 18	211 ± 36	20 ± 5
	OPN-CT	16 ± 3	64 ± 10	167 ± 26	19 ± 3
	OPN-NT	21 ± 2	187 ± 40	261 ± 42	14 ± 8
		Lower Chamber			
		PBS	OPN	OPN-CT	OPN-NT
Upper Chamber	PBS	56 ± 10	312 ± 56	478 ± 98	71 ± 21
	OPN	34 ± 7	168 ± 24	305 ± 50	36 ± 19
	OPN-CT	9 ± 4	88 ± 18	220 ± 38	26 ± 5
	OPN-NT	63 ± 11	287 ± 60	409 ± 55	14 ± 5
		Upper Surface			
	OPN (μg)	0	1	3	5
Lower Surface	0	1 ± 0.15	1.5 ± 0.2	1.8 ± 0.1	0.6 ± 0.2
	1	5.2 ± 0.35	1.5 ± 0.3		
	3	7.8 ± 0.4		2.1 ± 0.3	
	5	9.3 ± 0.8			2.0 ± 0.1
		Haptotactic index			Chemotactic index
Control		1 ± 0.3			1 ± 0.2
nOPN		9.8 ± 0.9			13.3 ± 1.9
+1 mM GRGDS		3.6 ± 1.0			10.6 ± 1.3
+1 mM GDPRS		9.6 ± 1.2			10.2 ± 2.1
+0.1 μg anti-integrin β-3		4.8 ± 0.6			9.8 ± 0.6
nOPN-NT		6.1 ± 0.7			
+1 mM GRGDS		2.1 ± 0.2			
+0.1 μg anti-CD44		5.5 ± 0.3			
+0.1 μg anti-integrin β-3		1.6 ± 0.1			
OPN-CT					9.6 ± 1.9
+1 mM GRGDS					7.7 ± 1.6
+0.1 μg anti-CD44					4.6 ± 0.7
+0.1 μg anti-integrin β-3					12.1 ± 2.1

only data from experiments with greater than 95% cell viability were used. Further, under the conditions used in these experiments, cell attachment was temperature-dependent, inhibitable by trypsin treatment, and not affected by inhibitors of protein synthesis or secretion. Cell spreading was determined by membrane-contour analysis and was scored according to increase in cell volume/surface area. In some experiments, cell spreading was also assessed by the formation of stress fibers. Each experiment was performed in quadruplicate wells and repeated three times.

Zymography

Secretion of proteinases was assayed by sodium dodecyl sulfate (SDS)-substrate gel electrophoresis under nonreducing conditions as described [44, 45]. Cell culture supernatant was collected after 6 h of culture, concentrated five times, and resuspended in 200 μl zymogram buffer (40 mM Tris, pH 7.5) before addition to Laemmli sample buffer and electrophoresis in 10% polyacrylamide gels, impregnated with 1 mg/ml gelatin. Following electrophoresis, gels were incubated for 30 min at 37°C in 50 ml 50 mM Tris-HCl buffer, pH 8.0, containing 2% Triton X-100 and 10 mM CaCl₂ to remove the SDS, followed by incubation for 18 h in 50 mM Tris-HCl buffer, pH 8.0, containing 5 mM CaCl₂. After staining the gels with Coomassie brilliant blue, gelatin-

degrading enzymes were identified as clear bands against a dark blue background.

RESULTS

Osteopontin interacts with CD44⁺ and CD44⁻ macrophages in vivo

Singh et al. [16] have reported an RGD-dependent interaction between osteopontin and integrin receptors and in vivo attraction of macrophages by subcutaneously injected osteopontin. We analyzed osteopontin-attracted macrophage populations for expression of CD44. Titration of soluble osteopontin into the peritoneum resulted in a dose-dependent increase in the cellular infiltrate (**Fig. 1, A and B**). According to our preliminary experiments, the peak response occurred at 4–6 h at about 10 μg osteopontin; the decreased response after 6 h may reflect

TABLE 1. (Continued)

	Haptotactic index	Chemotactic index
Control	1 ± 0.3	1 ± 0.2
rOPN	1.5 ± 0.1	10.5 ± 2.2
nOPN dephos.	3.6 ± 0.6	11.4 ± 1.8
PrOPN (PKA)	1.3 ± 0.2	9.6 ± 0.7
PrOPN (PKG)	0.8 ± 0.4	8.7 ± 2.0
PrOPN (CKI)	10.0 ± 1.9	9.9 ± 2.3
PrOPN (CKII)	8.0 ± 1.8	10.3 ± 1.6
PrOPN (GK)	12.6 ± 2.1	10.4 ± 1.6
nOPN	9.8 ± 0.9	13.3 ± 1.9
rOPN-CT	1.3 ± 0.6	9.6 ± 1.9
nOPN-CT	1.6 ± 0.5	9.6 ± 1.9
rOPN-NT	0.6 ± 0.2	0.9 ± 0.2
nOPN-NT	6.1 ± 0.7	0.9 ± 0.1
rOPN-NT10k	1.8 ± 0.9	1.1 ± 0.1
nOPN-NT10k	4.2 ± 1.1	1.1 ± 0.2

(A) Chemotaxis of A31.C1 cells, stably transfected with CD44. Soluble osteopontin (OPN) or its cleavage fragments were added to the lower well of a Boyden chamber in the presence or absence of equal amounts of osteopontin or its fragments in the upper well. Values are expressed as total numbers of transmigrated cells (mean ± SE); numbers in bold are significantly different from control values, with $P < 0.01$ or better. Numbers in italics are significantly different from the value in the top row of the column (reflecting inhibition of maximally induced migration), with $P < 0.05$ or better. (B) Chemotaxis of MH-S cells. Soluble osteopontin or its cleavage fragments were added to the Boyden chamber as described in A. Values are expressed as total numbers of transmigrated cells (mean ± SE); numbers in bold are significantly different from control values, with $P < 0.01$ or better. Numbers in italics are significantly different from the value in the top row of the column (reflecting inhibition of maximally induced migration), with $P < 0.05$ or better. (C) Haptotactic response of MH-S cells. The lower side of the transwell membrane was coated with increasing amounts of osteopontin in the presence or absence of increasing amounts of osteopontin on the upper side of the transwell membrane. Data are expressed as migratory index (cells migrating in response to osteopontin/cells migrating in response to buffer). Values are expressed as mean ± SE; numbers in bold are significantly different from control values, with $P < 0.01$ or better. (D and E) Middle columns: Haptotaxis of MH-S cells across polycarbonated filters in response to osteopontin (300 pmoles) bound to the lower surface. In controls wells, coated filters were placed into the Boyden chamber with the coated side up or with both sides coated (compare C). Right columns: Chemotactic activity was tested with soluble osteopontin (300 nM) in the lower chamber. Monocyte migration was mainly directional (i.e., the cells responded to a positive gradient of osteopontin; compare A and B). (D) Purified, natural osteopontin (nOPN) exerted chemotactic and haptotactic activity for the MH-S monocyte cell line through distinct domains, which were differentially inhibited by modulators of integrin binding (GRGDS peptide, anti-integrin β_3 antibody 2C9.G2) or CD44 binding (antibody KM81, clone TIB 241). The antibody concentrations used were saturating in a preliminary experiment as judged by titration of anti-integrin β_3 antibody (haptotactic indices 9.8 at 0 μg , 2.0 at 0.1 μg , 2.2 at 0.2 μg , 2.2 at 0.5 μg) and anti-CD44 (chemotactic indices 13.3 at 0 μg , 4.9 at 0.1 μg , 4.4 at 0.5 μg , 5.1 at 1 μg , 4.3 at 2 μg). (E) Recombinant osteopontin (rOPN) was phosphorylated with the indicated kinases as previously described [30, 40–42]. rOPN (GK), rOPN phosphorylated with Golgi kinases isolated from mouse calvarial cells (14 mol phosphate/mol protein); rOPN (CKII), rOPN phosphorylated with casein kinase II (9 mol phosphate/mol protein); rOPN (CKI), rOPN phosphorylated with casein kinase I (11 mol phosphate/mol protein); rOPN (PKA), rOPN phosphorylated with cyclic adenosine monophosphate (cAMP)-dependent kinase (low incorporation of phosphate); rOPN (PKG), rOPN phosphorylated with cGMP-dependent protein kinase (3 mol phosphate/mol protein); OPN-NT10k, N-terminal 10-kD fragment of osteopontin. As phosphorylation at any site never reaches 100%, the mol phosphate/mol protein underestimates the total number of sites phosphorylated. Data are expressed as migratory index (cells migrating in response to osteopontin/cells migrating in response to buffer). Values are expressed as mean ± SE; numbers in bold are significantly different from control values, with $P < 0.05$ or better. Similar results were obtained with MT-2/I cells (not shown).

clearance of soluble osteopontin from the peritoneal cavity. The numbers of Mac-1⁺ cells in the infiltrate were increased fivefold over basal levels and about 90% of peritoneal macrophages were CD44⁺. Osteopontin injections induced a disproportionately high increase in Mac-1⁺CD44⁺ (5.27 ± 1.14-fold at 10 μg osteopontin) as well as Mac-1⁺CD44⁻ cells (6.27 ± 2.28-fold), implying that ligation of both classes of osteopontin receptors may contribute to migration in vivo. The predominant migration of Mac-1⁺ cells (about 65% of the infiltrate) is consistent with previous studies of osteopontin [16] and is in contrast to the inflammatory response to lipopolysaccharide (LPS), which consists of roughly equal numbers of CD3⁺, B220⁺, and Mac-1⁺ cells (data not shown). This cellular infiltration is unlikely to reflect contamination of osteopontin, which was pure according to peptide sequence analysis, as coinjection of osteopontin with anti-osteopontin antibody prevented the influx of cells, whereas rabbit immunoglobulin had no effect (data not shown).

Our previous investigations of stable transfectants of A31 cells indicated that the interaction of osteopontin with CD44

depended on expression of CD44 splice variants 3–6 [14], which characterize activated lymphocytes [46]. More recent studies indicate that A31 cells transfected with the standard form of CD44 (lacking variant exons) do not bind osteopontin (unpublished results and ref. [47]). These findings are consistent with the observation that lymphocytes attracted into the peritoneal cavity appear to be activated as judged by increased forward-scatter measurements in flow cytometry.

The C-terminal domain of osteopontin interacts with CD44 to induce chemotaxis

Earlier studies of osteopontin binding to the myelomonocytic cell line Wehi 3 suggested that this interaction depended mainly on engagement of integrin receptors [16], and later investigations identified CD44 as a second receptor that was associated with chemotaxis [14]. As thrombin cleaves osteopontin in two sites releasing two large fragments, an N-terminal 1–153 fragment containing the RGD motif and a 158–294 C-terminal fragment [33], and as previous studies have demonstrated that the attachment of tumor cells is medi-

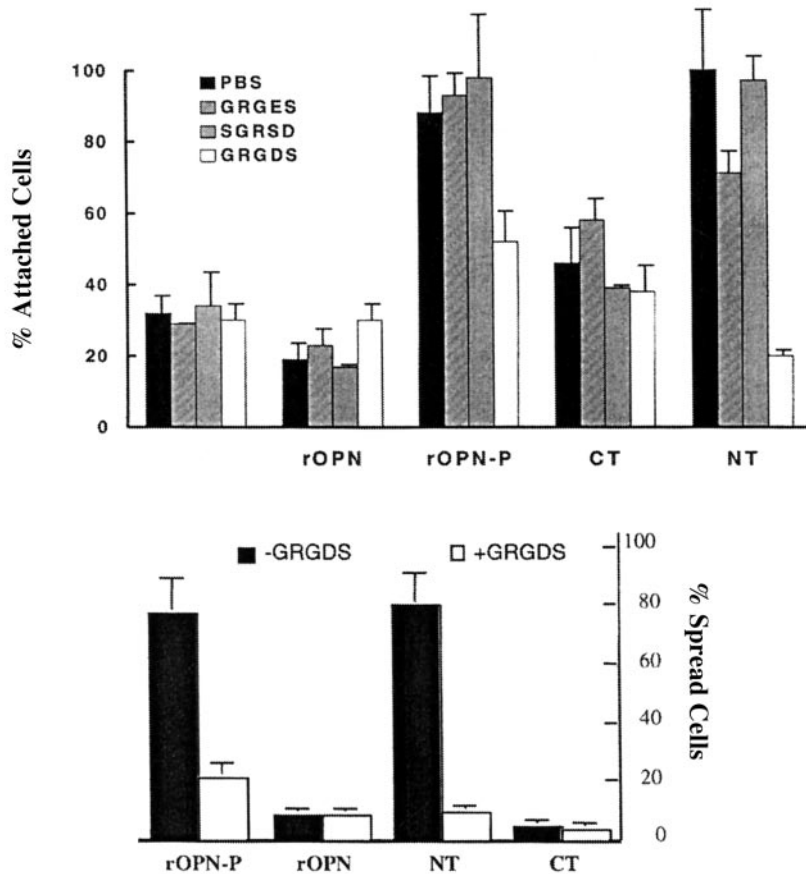
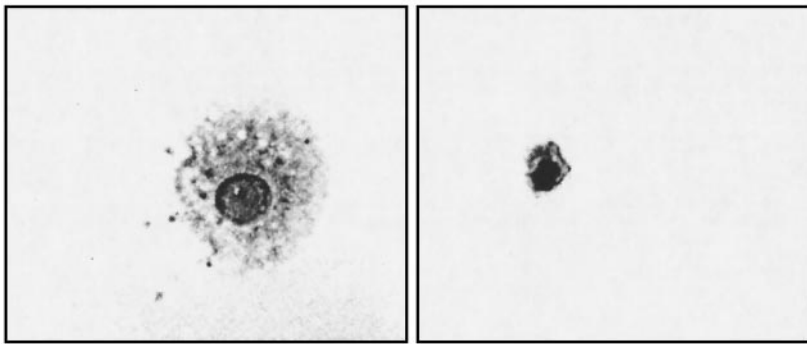


Fig. 3. Phosphorylation of osteopontin is required to induce cell spreading. MH-S monocytic cells (10^3 /well) or MT-2/1 cells (not shown) were incubated in 96-well plates that had been coated with $10 \mu\text{g/ml}$ (300 nM) indicated ligands for 1 h before washing, staining with toluidine blue, and counting. (Top) Change in cell morphology: MH-S cells attached to and spread on immobilized phosphorylated osteopontin; MH-S cells bound to unphosphorylated osteopontin do not spread (original magnification, $400\times$). (Middle) Numbers of cells attached to the indicated ligands in the presence or absence of GRGDS peptide or of the control peptides GRGES or SGRSD. Values are expressed as mean \pm SE. (Bottom) Numbers of cells spread on the indicated ligands in the presence or absence of GRGDS. Values are expressed as mean \pm SE. rOPN, Recombinant osteopontin; -P, native, phosphorylated osteopontin; -, no osteopontin; NT, N-terminal thrombin cleavage fragment of osteopontin; CT, C-terminal fragment.

ated preferentially by RGD-containing domains of osteopontin [48], we exploited these observations to determine whether distinct domains of osteopontin were responsible for engagement of the two receptors. The macrophage cell lines MT-2/1 and MH-S express the relevant receptors, integrin β_3 and CD44, at high levels according to flow cytometry. Although one form containing variant exons appears to be the most prominent CD44 gene product as judged by PCR with primers for the constitutive exons 5 and 16, three bands between 200 and 400 base pairs are amplified with primers for exon 5 and exon v6. Expression of standard CD44 was not detected (**Fig. 2**).

The CD44-transfected cell line A31.C1 migrated toward soluble osteopontin or the C-terminal fragment but not toward the N-terminal fragment (**Table 1A**). The vector-transfected control does not chemotax toward osteopontin [14], confirming that the C-terminal domain of osteopontin interacts with CD44. The C-terminal fragment of osteopontin also induced chemo-

taxis of the macrophage cell line MH-S as efficiently as intact osteopontin, and the N-terminal, 30-kDa osteopontin fragment was inactive (**Table 1, B-E**); equimolar mixtures of both fragments displayed activity similar to that of the 28-kDa C-terminal fragment alone (data not shown). Chemotaxis induced by osteopontin or its C-terminal domain was inhibitable by anti-CD44 antibody but not by GRGDS peptide or anti-integrin β_3 antibody. These results, taken together, indicate that the 28-kDa C-terminal part of the molecule is sufficient to induce CD44-dependent chemotaxis.

The N-terminal domain of osteopontin induces haptotaxis of macrophages via integrin β_3

Cells can move up a gradient of immobilized ligand; this cell-crawling may occur on vessel walls or in the interstitium and is referred to as haptotaxis. We assessed the contribution

of interactions between immobilized osteopontin and integrin receptors to cell motility. The ability of the immobilized ligand to induce monocyte haptotaxis was judged by cell migration through polycarbonate filters. Osteopontin induced monocyte migration that was mainly directional (i.e., the cells responded to a positive gradient of bound osteopontin; Table 1C) and thus haptotactic and was inhibited by GRGDS and antibody to the β_3 chain of integrins but not by antibody to CD44 (Table 1D).

As some osteopontin functions are dependent on the phosphorylation of the ligand, we attempted to localize the critical residues for haptotaxis. Phosphorylation has to occur at specific sites, as Golgi kinases and casein kinase I or II can activate osteopontin, whereas protein kinase A or G phosphorylates the recombinant molecule but does not confer integrin binding (Table 1E). Earlier studies, which showed that RGD-containing peptides can confer function, may have induced nonspecific effects through multiple integrin receptors. Our data demonstrate that the RGD motif is necessary but not sufficient to confer specific osteopontin function; a sequence N-terminal to the RGD sequence is also needed.

The N-terminal domain of osteopontin induces spreading and activation of macrophages via integrin β_3

Macrophage spreading on extracellular matrix proteins depends, in part, on engagement of their integrin receptors. Spreading of the MH-S macrophage cell line on immobilized, native osteopontin is mediated by the RGD-containing N-terminal thrombin cleavage fragment but not by the C-terminal fragment and is reversed by addition of soluble GRGDS but not control GRGES peptide. Moreover, phosphorylation of recombinant osteopontin is required for this activity (Fig. 3).

Osteopontin induces proinflammatory mediators through integrin β_3

Macrophage spreading is often associated with cellular activation. Here, we analyze the effects of osteopontin on macrophage production of effector cytokines including several proinflammatory mediators and metalloproteinases. Metalloproteinases, which regulate cell motility and invasion, represent a family of more than 14 proteolytic enzymes that have distinct but overlapping substrate specificity. Metalloprotease 2 and 9 cleave type IV collagen and are thought to be essential for efficient migration of monocytes through basement membranes. The phosphorylated N-terminal fragment but not the C-terminal fragment of osteopontin induced strong MMP-9 (gelatinase B) responses (Fig. 4), and induction was inhibited by GRGDS but not GRGES (data not shown). Consistent with its role in delayed-type hypersensitivity responses, osteopontin induced interleukin (IL)-12 and tumor necrosis factor α (TNF- α) but not IL-1 β , IL-10, or IL-6. Additional analysis revealed that cytokine induction depends on the interaction between phosphorylated osteopontin and peritoneal macrophages (Fig. 5). This interaction was mediated by the N-terminal portion of osteopontin and was inhibited by GRGDS and integrin β_3 antibody (not shown).

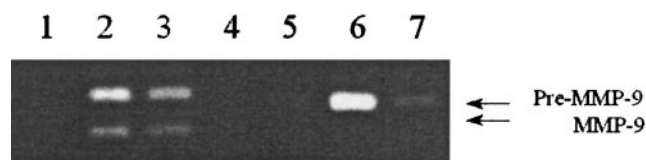


Fig. 4. Induction of metalloprotease secretion by phosphorylated but not unphosphorylated osteopontin. MH-S cells were stimulated for 6 h with phosphorylated or unphosphorylated osteopontin at a concentration of 10 μ g/ml (300 nM) in serum-free, defined medium. To visualize the secreted metalloproteases, gelatin zymograms were performed. MMP-9 and pre-MMP-9 are visible in the sample stimulated with natural osteopontin (lane 2) and samples stimulated with phosphorylated recombinant osteopontin (lane 3). Dephosphorylation of osteopontin with acid phosphatase abolishes the stimulatory activity of osteopontin (lane 4). Similarly, recombinant osteopontin has no stimulatory activity (lane 5). The pre-form but not active MMP9 is stimulated by the N-terminal fragment of osteopontin (lane 6), and the C-terminal fragment of osteopontin has little or no stimulatory activity (lane 7). Control, MH-S cells were incubated with serum-free, defined medium (lane 1).

DISCUSSION

The present structure-function analysis of osteopontin demonstrates that engagement of its two main receptors by distinct domains leads to differential monocyte responses. Chemoattractant activity resides within the C-terminal region of osteopontin and is mediated by CD44. In contrast, the RGD motif within a nonoverlapping N-terminal portion of osteopontin, exposed after phosphorylation or thrombin cleavage, can induce haptotaxis and cellular activation. Thus, in addition to the well-established role of phosphorylation in regulating the biological interactions of intracellular enzymes and their substrates, phosphorylation of a secreted extracellular protein also can provide molecular information that targets it to particular interaction partners, which dictate its biological activity. In vivo, additional components may contribute to regulating osteopontin biology. Several other integrin receptors are engaged by osteopontin [13, 21]. Furthermore, CD44 may be ligated individually or in association with integrin β_1 [47]. This interaction is not likely to contribute to chemotaxis, as the integrin β_1 -binding sites on osteopontin have been mapped outside the C-terminal fragment used in our experiments; however, other in vivo functions by coligated CD44 and integrin β_1 are possible. The combined contributions by all receptors may underlie the profound effects of osteopontin on cellular immunity.

The participation of monocytes/macrophages in inflammation entails emigration of these cells from peripheral blood into infected tissues, where they produce cytokines that regulate diverse processes including antimicrobial activity, cell growth, differentiation, and wound healing [49]. Emigration of monocytes depends on coordinate engagement of different subsets of cell surface receptors by cytokines and extracellular matrix that underlie migration or adhesion within various anatomic compartments. Osteopontin plays an important role in macrophage infiltration in response to pathological stimuli [50]. Our findings suggest that attraction and activation of monocytes depend, in part, on orchestrated activities of osteopontin-binding domains that have been modified by thrombin [22], ectokinases [51], and ecto-phosphatases [32]. Thrombin cleavage of osteopontin that has been integrated into the matrix through

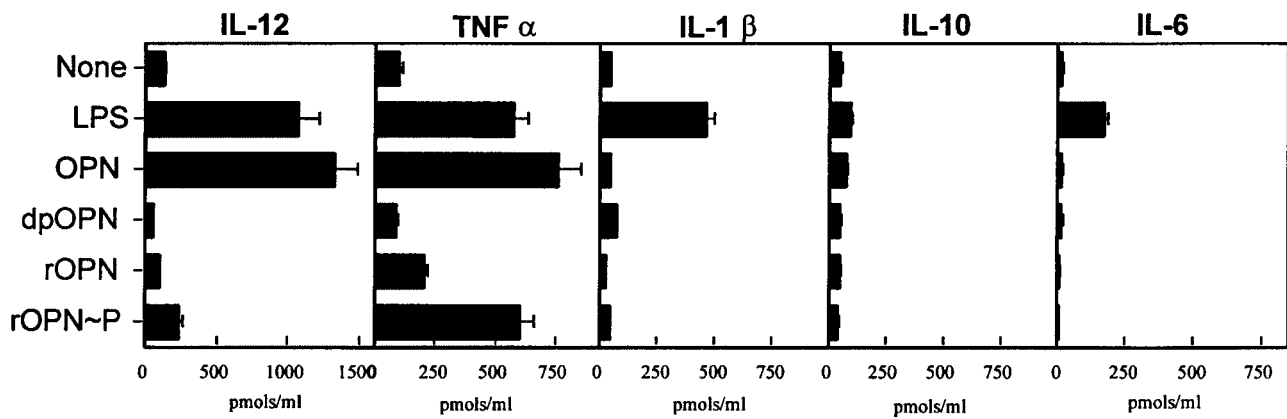


Fig. 5. Osteopontin induces secretion of inflammatory mediators from macrophages. Resident peritoneal macrophages, obtained by peritoneal lavage with PBS, were treated with red cell lysis buffer and incubated (10^5 macrophages per 100 μ l) for 2 h. The adherent fraction was incubated with 5 nM osteopontin (OPN, native osteopontin; dpOPN, dephosphorylated native osteopontin; rOPN, recombinant osteopontin; rOPN~P, recombinant osteopontin phosphorylated by Golgi kinases) or 30 ng/ml LPS. Supernatant IL-12, TNF- α , IL-1 β , IL-10, and IL-6 were assayed at 24 or 48 h post-stimulation with commercial enzyme-linked immunosorbent assay kits (R&D Systems, Minneapolis, MN). Similar results were obtained with the MH-S cell line.

transglutaminases [52] can lead to the release of a chemotactic C-terminal osteopontin fragment and attraction of monocytes to a site of infection. Subsequent engagement of integrin receptors on emigrant monocytes by the immobilized, phosphory-

lated N-terminal domain of osteopontin may facilitate local haptotactic migration toward a site of microbial infection or inflammation (**Fig. 6**). After arrival, attachment and spreading of emigrant monocytes mediated by engagement of $\alpha_v\beta_3$ inte-

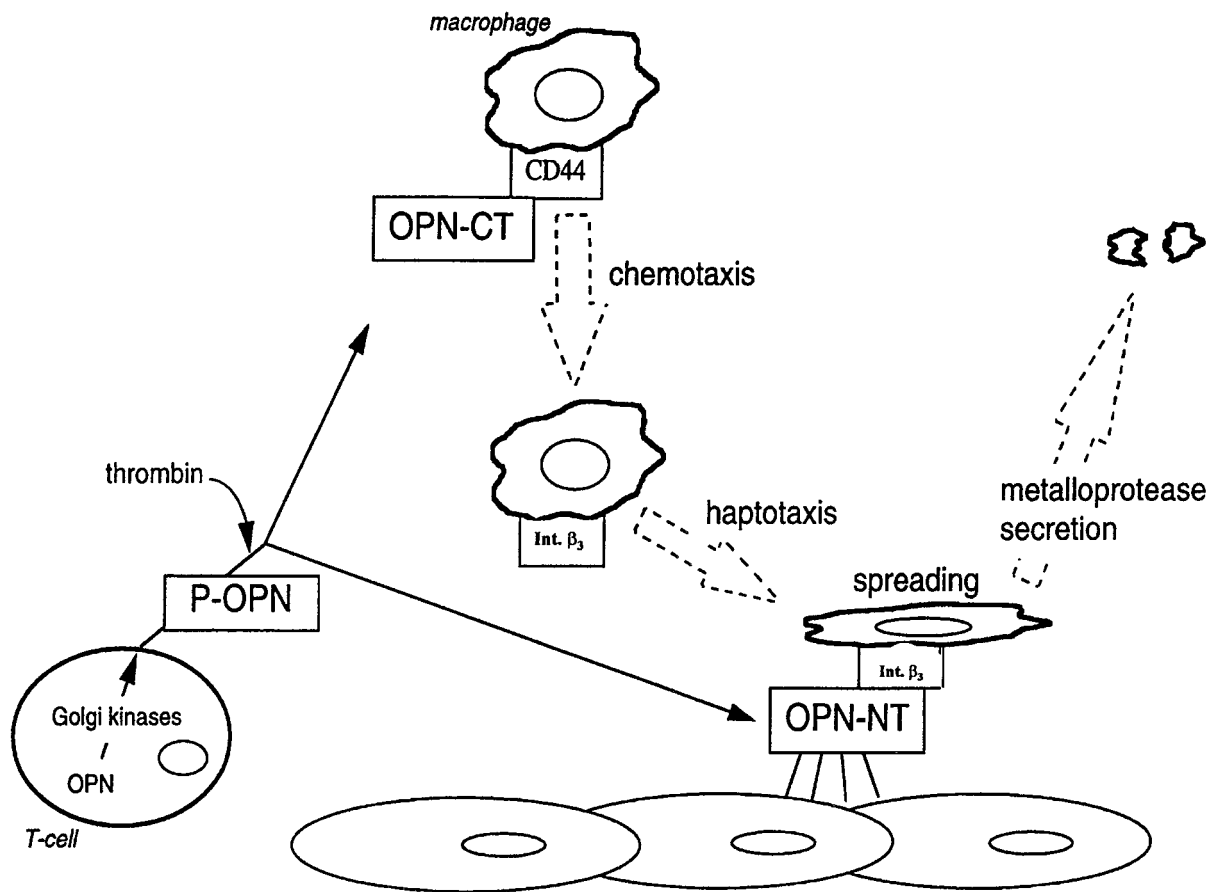


Fig. 6. Model of monocyte regulation by osteopontin. Osteopontin is secreted by activated T cells. Thrombin cleavage releases the two receptor-binding domains, which carry out distinct functions in the cascade of events leading to macrophage attraction and activation. The C-terminal piece exerts chemotactic activity that is phosphorylation-independent, leading to attraction of macrophages to the cleavage site and cellular attachment to the osteopontin N-terminal fragment. Phosphorylation-dependent haptotaxis on cross-linked osteopontin or OPN-NT leads to macrophage spreading and activation, including induction of cytokine secretion and release of metalloproteases that can degrade the matrix.

grin receptors by the N-terminal osteopontin thrombin cleavage product (possibly through increased access of the RGD-binding site; ref. [19]) can lead to macrophage activation and expression of inflammatory mediators such as metalloproteases and cytokines (Fig. 5). The cytokine profile reflects a type 1 pattern and in conjunction with the coordinated regulation of macrophage migration and invasion, accounts for the prominent role played by the cytokine osteopontin in cellular immunity [35]. The coupling of macrophage cell shape and gene expression through the linkage of cytoskeletal networks to the extracellular matrix provides a molecular framework for differential responses to various presentations of the same ligand [53]. Although additional *in vivo* studies are required to test this model, the definition of the functional domains of osteopontin in this report represents an important step in understanding this process and may allow the rational development of osteopontin analogs that antagonize or mimic discrete biological activities of the parent molecule.

ACKNOWLEDGMENTS

This study was supported in part by the National Institutes of Health (NIH): AI12184 to H. C.; CA76176 to G. F. W.; Department of Defense (DOD) breast cancer grant DAMD 17-98-1-8060 to G. F. W. and DAMD-17-99-1-9124 to S. A.; and Department of Public Health Grant 340B9930002 and OraPharma to S. A. S. Z. is supported by a grant from the Fullbright Foundation. Dr. Paola Riccardi-Castagnoli generously provided the MT-2 cells. The authors are grateful to Lisa Lagasse and Alison Angel for assistance in the preparation of the manuscript.

REFERENCES

- Patarca, R., Freeman, G. J., Singh, R. P., Wei, F.-Y., Durfee, T., Blattner, F., Regnier, D. C., Kozack, C. A., Mock, B. A., Morse III, H. C., Jerrells, T. R., Cantor, H. (1989) Structural and functional studies of the early T lymphocyte activation 1 (Eta-1) gene. Definition of a novel T cell-dependent response associated with genetic resistance to bacterial infection. *J. Exp. Med.* 170, 145–161.
- Patarca, R., Singh, R. P., Wei, F.-Y., Iregui, M. V., Singh, P., Schwartz, J., Cantor, H. (1990) Alternative pathways of T-cell activation and positive clonal selection. *Immunol. Rev.* 116, 1–16.
- Nau, G. J., Guilfoile, P., Chupp, G. L., Berman, J. S., Kim, S. J., Kornfeld, H., Young, R. A. (1997) A chemoattractant cytokine associated with granulomas in tuberculosis and silicosis. *Proc. Natl. Acad. Sci. USA* 94, 6414–6419.
- Yu, X. Q., Nikolic-Paterson, D. J., Mu, W., Giachelli, C. M., Atkins, R. C., Johnson, R. J., Lan, H. Y. (1998) A functional role for osteopontin in experimental crescentic glomerulonephritis in the rat. *Proc. Am. Assoc. Phys.* 110, 50–64.
- McKee, M. D., Nanci, A. (1996) Osteopontin: an interfacial extracellular matrix protein in mineralized tissues. *Connect Tissue Res.* 35, 197–205.
- Nakase, T., Sugimoto, M., Sato, M., Kaneko, M., Tomita, T., Sugamoto, K., Nomura, S., Kitamura, Y., Yoshikawa, H., Yasui, N., Yonenobu, K., Ochi, T. (1998) Switch of osteonectin and osteopontin mRNA expression in the process of cartilage-to-bone transition during fracture repair. *Acta Histochem.* 100, 287–295.
- Wang, X., Loudon, C., Yue, T. L., Ellison, J. A., Barone, F. C., Solleveld, H. A., Feuerstein, G. Z. (1998) Delayed expression of osteopontin after focal stroke in the rat. *J. Neurosci.* 18, 2075–2083.
- Liaw, L., Birk, D. E., Ballas, C. B., Whitsitt, J. S., Davidson, J. M., Hogan, B. L. (1998) Altered wound healing in mice lacking a functional osteopontin gene (spp1). *J. Clin. Investig.* 101, 1468–1478.
- Giachelli, C. M., Liaw, L., Murry, C. E., Schwartz, S. M., Almeida, M. (1995) Osteopontin expression in cardiovascular diseases. *Ann. N. Y. Acad. Sci.* 760, 109–126.
- Oldberg, A., Franzen, A., Heinegard, D. (1986) Cloning and sequence analysis of rat bone sialoprotein (osteopontin) cDNA reveals an Arg-Gly-Asp cell-binding sequence. *Proc. Natl. Acad. Sci. USA* 83, 8819–8823.
- Oldberg, A., Franzen, A., Heinegard, D., Pierschbacher, M. D., Ruohslahhti, E. (1986) Identification of a bone sialoprotein receptor in osteosarcoma cells. *J. Biol. Chem.* 263, 19433–19436.
- Salih, E., Ashkar, S., Gerstenfeld, L. C., Glimcher, M. J. (1996) Protein kinases of cultured osteoblasts: selectivity for the extracellular matrix proteins of bone and their catalytic competence for osteopontin. *J. Bone Miner. Res.* 11, 1461–1473.
- Liaw, L., Skinner, M. P., Raines, E. W., Ross, R., Cheresch, D. A., Schwartz, S. M., Giachelli, C. M. (1995) The adhesive and migratory effects of osteopontin are mediated via distinct cell surface integrins. Role of alpha v beta 3 in smooth muscle cell migration to osteopontin *in vitro*. *J. Clin. Investig.* 95, 713–724.
- Weber, G. F., Ashkar, S., Glimcher, M. J., Cantor, H. (1996) Receptor-ligand interaction between CD44 and osteopontin/Eta-1. *Science* 271, 509–512.
- van Dijk, S., D'Errico, J., Somerman, M. J., Farach-Carson, M. C., Butler, W. T. (1993) Evidence that a non-RGD domain in rat osteopontin is involved in cell attachment. *J. Bone Miner. Res.* 8, 1499–1506.
- Singh, R. P., Patarca, R., Schwartz, J., Singh, P., Cantor, H. (1990) Definition of a specific interaction between Eta-1 protein and murine macrophages *in vitro* and *in vivo*. *J. Exp. Med.* 171, 1931–1942.
- Liaw, L., Almeida, M., Hart, C. E., Schwartz, S. M., Giachelli, C. M. (1994) Osteopontin promotes vascular cell adhesion and spreading and is chemotactic for smooth muscle cells *in vitro*. *Circul. Res.* 74, 214–224.
- Denhardt, D. T., Guo, X. (1993) Osteopontin: a protein with diverse functions. *FASEB J.* 7, 1475–1482.
- Senger, D. R., Ledbetter, S. R., Claffey, K. P., Papadopoulos-Sergiou, A., Peruzzi, C. A., Detmar, M. (1996) Stimulation of endothelial cell migration by vascular permeability factor/vascular endothelial growth factor through cooperative mechanisms involving the beta 3 integrin, osteopontin, and thrombin. *Am. J. Pathol.* 149, 293–305.
- Yue, T. L., McKenna, P. J., Ohlstein, E. H., Farach-Carson, M. C., Butler, W. T., Johanson, K., McDevitt, P., Feuerstein, G. Z., Stadel, J. M. (1994) Osteopontin-stimulated vascular smooth muscle cell migration is mediated by beta 3 integrin. *Exp. Cell Res.* 214, 459–464.
- Nasu, K., Ishida, T., Setoguchi, M., Higuchi, Y., Akizuki, S., Yamamoto, S. (1995) Expression of wild type and mutated rabbit osteopontin in *Escherichia coli*, and their effects on adhesion and migration of P388D1 cells. *Biochem. J.* 307, 257–265.
- Senger, D. R., Perruzzi, C. A. (1996) Cell migration promoted by a potent GRGDS-containing thrombin cleavage fragment of osteopontin. *Biochim. Biophys. Acta* 1314, 13–24.
- Smith, L. L., Giachelli, C. M. (1998) Structural requirements for alpha 9 beta 1-mediated adhesion and migration to thrombin-cleaved osteopontin. *Exp. Cell Res.* 242, 351–360.
- Kubota, T., Zhang, Q., Wrana, J. L., Ber, R., Aubin, J. E., Butler, W. T., Sodek, J. (1989) Multiple forms of Spp1 (secreted phosphoprotein; osteopontin) synthesized by normal and transformed rat bone cell populations: regulation by TGF-alpha. *Biochem. Biophys. Res. Commun.* 162, 1453–1459.
- Chambers, A. F., Behrend, E. I., Wilson, S. M., Denhardt, D. T. (1992) Induction of expression of osteopontin in metastatic, ras-transformed NIH 3T3 cells. *Anticancer Res.* 12, 43–47.
- Barak-Shalom, T., Schickler, M., Knopov, V., Shapira, R., Hurwitz, S., Pines, M. (1995) Synthesis and phosphorylation of osteopontin by avian epiphyseal growth-plate chondrocytes as affected by differentiation. *Comp. Biochem. Physiol.* 111, 49–59.
- Chang, P. L., Prince, C. W. (1993) 1 alpha, 25-Dihydroxyvitamin D3 enhances 12-O-tetradecanoylphorbol-13-acetate-induced tumorigenic transformation and osteopontin expression in mouse JB6 epidermal cells. *Cancer Res.* 53, 2217–2220.
- Sorensen, E. S., Petersen, T. E. (1994) Identification of two phosphorylation motifs in bovine osteopontin. *Biochem. Biophys. Res. Commun.* 198, 200–205.
- Salih, E., Ashkar, S., Gerstenfeld, L. C., Glimcher, M. J. (1995) Identification of the *in vivo* phosphorylated sites of secreted osteopontin from chicken osteoblasts. *Ann. N. Y. Acad. Sci.* 760, 357–360.
- Salih, E., Ashkar, S., Gerstenfeld, L. C., Glimcher, M. J. (1997) Identification of the phosphorylated sites of metabolically ³²P-labeled osteopontin from cultured chicken osteoblasts. *J. Biol. Chem.* 272, 13966–13973.
- Nemir, M., DeVouge, M. W., Mukherjee, B. B. (1989) Normal rat kidney cells secrete both phosphorylated and nonphosphorylated forms of os-

- teopontin showing different physiological properties. *J. Biol. Chem.* 264, 18202–18208.
32. Ek-Rylander, B., Flores, M., Wendel, M., Heinegard, D., Andersson, G. (1994) Dephosphorylation of osteopontin and bone sialoprotein by osteoclastic tartrate-resistant acid phosphatase. Modulation of osteoclast adhesion in vitro. *J. Biol. Chem.* 269, 14853–14856.
 33. Senger, D. R., Brown, L. F., Peruzzi, C. A., Papadopoulos-Sergious, A., van der Water, L. (1995) Osteopontin at the tumor/host interface. Functional regulation by thrombin cleavage and consequences for cell adhesion. *Ann. N. Y. Acad. Sci.* 760, 83–100.
 34. Xuan, J. W., Hota, C., Shigeyama, Y., D'Errico, J. A., Somerman, M. J., Chambers, A. F. (1995) Site-directed mutagenesis of the arginine-glycine-aspartic acid sequence in osteopontin destroys cell adhesion and migration functions. *J. Cell. Biochem.* 57, 680–690.
 35. Ashkar, S., Weber, G. F., Panoutsakopoulou, V., Sanchirico, M. E., Janssen, M., Zawaideh, S., Rittling, S., Denhardt, D. T., Glimcher, M. J., Cantor, H. (2000) The cytokine Eta-1/Opn is an essential molecular bridge to type 1 (cell-mediated) immunity. *Science* 287, 860–864.
 36. Adler, B., Ashkar, S., Cantor, H., Weber, G. F. (2001) Costimulation by extracellular matrix proteins determines the response to TCR ligation. *Cell. Immunol.* 210, 30–40.
 37. Weber, G. F., Adler, B., Ashkar, S. (1999) Osteopontin in oxidative stress responses. In *Inflammatory Cells and Mediators in CNS Diseases* (R. R. Ruffolo Jr., G. Z. Feuerstein, A. J. Hunter, G. Poste, B. W. Metcalf, eds.), Amsterdam, Harwood Academic, 97–112.
 38. Lutz, M. B., Granucci, F., Winzler, C., Marconi, G., Paglia, P., Foti, M., Asmann, C. U., Cairns, L., Rescigno, M., Ricciardi-Castagnoli, P. (1994) Retroviral immortalization of phagocytic and dendritic cell clones as a tool to investigate functional heterogeneity. *J. Immunol. Methods* 174, 269–279.
 39. Stickeler, E., Kittrell, F., Medina, D., Berget, S. M. (1999) Stage-specific changes in SR splicing factors and alternative splicing in mammary tumorigenesis. *Oncogene* 18, 3574–3582.
 40. Ashkar, S., Glimcher, M. J., Saavedra, R. A. (1993) Mouse osteopontin expressed in *E. coli* autophosphorylates tyrosine residues. *Biochem. Biophys. Res. Commun.* 194, 274–279.
 41. Ashkar, S., Teplow, D. B., Glimcher, M. J., Saavedra, R. A. (1993) In vitro phosphorylation of mouse osteopontin expressed in *E. coli*. *Biochem. Biophys. Res. Commun.* 191, 126–133.
 42. Ashkar, S., Schaffer, J. L., Salih, E., Gerstenfeld, L. C., Glimcher, M. J. (1995) Phosphorylation of osteopontin by Golgi kinases. *Ann. N. Y. Acad. Sci.* 760, 296–298.
 43. Moses, M. A., Sudhalter, J., Langer, R. (1990) Identification of an inhibitor of neovascularization from cartilage. *Science* 248, 1408–1410.
 44. Giunciuglio, D., Cai, T., Filanti, C., Manduca, P., Albini, A. (1995) Effect of osteoblast supernatants on cancer cell migration and invasion. *Cancer Lett.* 97, 69–74.
 45. Umemori, E. N., Werb, Z. (1986) Reorganization of polymerized actin: a possible trigger for induction of procollagenase in fibroblasts cultured in and on collagen gels. *J. Cell Biol.* 103, 1021–1031.
 46. Arch, R., Wirth, K., Hofmann, M., Ponta, H., Matzku, S., Herrlich, P., Zoeller, M. (1992) Participation in normal immune responses of a meta-static inducing splice variant of CD44. *Science* 257, 682–685.
 47. Katagiri, Y. U., Sleeman, J., Fujii, H., Herrlich, P., Hotta, H., Tanaka, K., Chikuma, S., Yagita, H., Okumura, K., Murakami, M., Saiki, I., Chambers, A. F., Ueda, T. (1999) CD44 variants but not CD44s cooperate with beta1-containing integrins to permit cells to bind to osteopontin independently of arginine-glycine-aspartic acid, thereby stimulating cell motility and chemotaxis. *Cancer Res* 59, 219–226.
 48. Xuan, J. W., Hota, C., Chambers, A. F. (1994) Recombinant GST-human osteopontin fusion protein is functional in RGD-dependent cell adhesion. *J. Cell. Biochem.* 54, 247–255.
 49. Singer, I. I., Kawka, D. W., Bayne, E. K., Donatelli, S. A., Weidner, J. R., Williams, H. R., Ayala, J. M., Mumford, R. A., Lark, M. W., Glant, T. T., et al. (1995) VDIPEN, a metalloproteinase-generated neopeptide, is induced and immunolocalized in articular cartilage during inflammatory arthritis. *J. Clin. Investig.* 95, 2178–2186.
 50. Giachelli, C. M., Lombardi, D., Johnson, R. J., Murry, C. E., Almeida, M. (1998) Evidence for a role of osteopontin in macrophage infiltration in response to pathological stimuli in vivo. *Am. J. Pathol.* 152, 353–358.
 51. Zhu, X. L., Luo, C., Ferrier, J. M., Sodek, J. (1997) Evidence of ectokinase-mediated phosphorylation of osteopontin and bone sialoprotein by osteoblasts during bone formation in vitro. *Biochem. J.* 323, 637–643.
 52. Mukherjee, B. D., Nemir, M., Beninati, S., Cordella-Miele, E., Singh, K., Chackalaparampil, I., Shanmugam, V., DeVouge, M. W., Mukherjee, A. B. (1995) Interaction of osteopontin with fibronectin and other extracellular matrix molecules. *Ann. N. Y. Acad. Sci.* 760, 201–212.
 53. Singhvi, R., Kuman, A., Lopez, G. P., Stephanopoulos, G. N., Wang, D. L., Whitesides, G. M., Ingber, D. E. (1994) Engineered cell shape and function. *Science* 264, 696–698.